

Cross-Platform Verification of Intermediate Scale Quantum Devices

Andreas Elben¹, Benoît Vermersch, Rick van Bijnen, Christian Kokail, Tiff Brydges, Christine Maier, Manoj K. Joshi, Rainer Blatt, Christian F. Roos, and Peter Zoller
Center for Quantum Physics, University of Innsbruck, Innsbruck A-6020, Austria and Institute for Quantum Optics and Quantum Information of the Austrian Academy of Sciences, Innsbruck A-6020, Austria

 (Received 3 September 2019; published 6 January 2020)

We describe a protocol for cross-platform verification of quantum simulators and quantum computers. We show how to measure directly the overlap $\text{Tr}[\rho_1\rho_2]$ and the purities $\text{Tr}[\rho_{1,2}^2]$, and thus a fidelity of two, possibly mixed, quantum states ρ_1 and ρ_2 prepared in separate experimental platforms. We require only local measurements in randomized product bases, which are communicated classically. As a proof of principle, we present the measurement of experiment-theory fidelities for entangled 10-qubit quantum states in a trapped ion quantum simulator.

DOI: 10.1103/PhysRevLett.124.010504

There is an ongoing effort to build intermediate scale quantum devices involving several tens of qubits [1]. Engineering and physical realization of quantum computers and quantum simulators are being pursued with different physical platforms ranging from atomic and photonic to solid-state systems. Recently, verification procedures [2], such as randomized and cyclic benchmarking [3–7], and direct fidelity estimation [8–10] have been developed, which allow one to compare an implemented, noisy quantum process (or state) with a known, theoretical target. A key challenge is the direct comparison of *a priori* unknown quantum states generated on two devices at different locations and times by running a specific quantum computation or quantum simulation, i.e., the cross-platform verification of these experimental quantum devices by means of a fidelity measurement. This will become particularly relevant when we approach regimes where eventually a comparison with classical simulations becomes computationally hard and thus a direct comparison of quantum machines is needed.

Our aim is the development of protocols for cross-platform verification by measuring the overlap of quantum states produced with two different experimental setups, potentially realized on very different physical platforms, without any prior assumptions on the quantum states themselves. For two pure quantum states, the relevant fidelity is defined as the overlap $\mathcal{F}_{\text{pure}}(|\psi_1\rangle, |\psi_2\rangle) = |\langle\psi_1|\psi_2\rangle|^2$, where $|\psi_1\rangle$ and $|\psi_2\rangle$ denote pure states in Hilbert space \mathcal{H} on devices 1 and 2, respectively. For mixed states we consider the fidelity [11]

$$\mathcal{F}_{\text{max}}(\rho_1, \rho_2) = \frac{\text{Tr}[\rho_1\rho_2]}{\max\{\text{Tr}[\rho_1^2], \text{Tr}[\rho_2^2]\}}, \quad (1)$$

which measures the overlap between density matrices ρ_1 and ρ_2 , respectively, normalized by their purities. Here

ρ_1 (ρ_2) can refer to the total system, or a subsystem of device 1 (2). \mathcal{F}_{max} fulfills the axioms for mixed state fidelities imposed by Josza [12]. It can thus be used to verify that, and to which degree, two quantum devices have prepared the same quantum state. We note that the performance of quantum devices has been previously investigated by comparing outcome distributions of a selection of observables [13,14]. In contrast, we are interested here in specifically measuring the fidelity (1) of the entire density matrices ρ_1 and ρ_2 .

The protocol discussed below infers the cross-platform fidelity \mathcal{F}_{max} from statistical correlations between randomized measurements performed on the first and second device (see Fig. 1). While in previous work we obtained Rényi (entanglement) entropies, or purities, of reduced density matrices $\text{Tr}[\rho_{1,2}^2]$, for single systems from randomized measurements [15–17] [see the denominator of Eq. (1)], we are here interested in measuring the overlap between density operators of devices 1 and 2 from such protocols [see numerator of Eq. (1)]. In principle, \mathcal{F}_{max} can be determined from full quantum state tomography (QST) of systems 1 and 2 [10,18–22]. However, due to the exponential scaling with the (sub)system size [19], this approach is limited to only a few degrees of freedom [18]. Alternative efficient tomographic methods require a specific structure, or *a priori* knowledge of the system of interest [10,21–23]. In contrast, as demonstrated below, the present protocol scales, although exponentially, much more favorably with the (sub)system size, allowing practical cross-platform verification for (sub)systems involving tens of qubits on state-of-the-art quantum devices [24].

In the following, we first describe the protocol, followed by an analysis of statistical errors and the required number of experimental runs. Using the data taken in the context of Ref. [28], we demonstrate, as a proof of principle, the measurement of experiment-theory fidelities of quantum

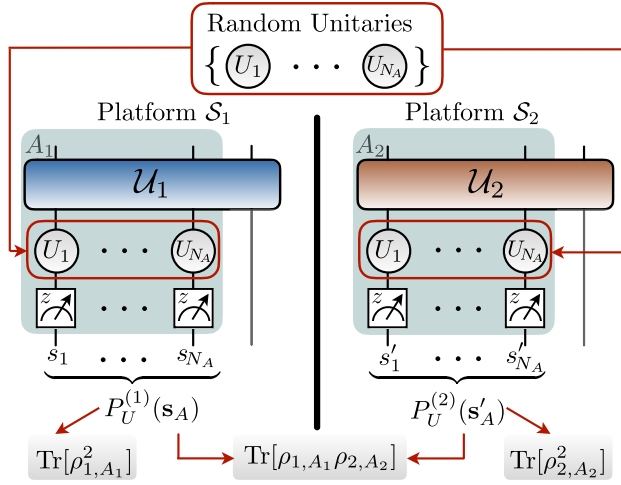


FIG. 1. Fidelity estimation with randomized measurements. We present a protocol to measure the fidelity $\mathcal{F}_{\max}(\rho_{1,A_1}, \rho_{2,A_2})$ of two quantum states described by (reduced) density matrices $\rho_{i,A_i} = \text{Tr}_{\mathcal{S}_i \setminus A_i}[\rho_i]$ ($i = 1, 2$). On two platforms \mathcal{S}_1 and \mathcal{S}_2 , the quantum states ρ_1 and ρ_2 are prepared with quantum operations \mathcal{U}_1 and \mathcal{U}_2 , respectively. Randomized measurements are performed on both platforms in (sub)systems $A_1 \subseteq \mathcal{S}_1$ and $A_2 \subseteq \mathcal{S}_2$ of size N_A , implemented with the *same* local random unitaries $U_1 \otimes \dots \otimes U_{N_A}$ which are shared via classical communication (red arrows). From statistical cross-correlations (autocorrelations) of outcome probabilities $P_U^{(i)}(\mathbf{s}_A)$ ($i = 1, 2$), the overlap $\text{Tr}[\rho_{1,A_1} \rho_{2,A_2}]$ (the purities $\text{Tr}[\rho_{i,A_i}^2]$) and thus $\mathcal{F}_{\max}(\rho_{1,A_1}, \rho_{2,A_2})$ are inferred (see text).

states of 10 qubits prepared via quench dynamics on a trapped ion quantum simulator. Finally, we present experiment-experiment fidelities of quantum states prepared sequentially on the same experimental platform.

Protocol.—As illustrated in Fig. 1, we consider two quantum devices consisting of N_1 and N_2 spins (d -level systems) realized on different physical platforms \mathcal{S}_1 and \mathcal{S}_2 , and prepared with quantum operations \mathcal{U}_1 and \mathcal{U}_2 in two quantum states described by the density matrices ρ_1 and ρ_2 , respectively. We denote the reduced density matrices as $\rho_{i,A_i} = \text{Tr}_{\mathcal{S}_i \setminus A_i}(\rho_i)$ for (sub) systems $A_i \subseteq \mathcal{S}_i$ ($i = 1, 2$) of identical size $N_{A_1} = N_{A_2} \equiv N_A$. The associated Hilbert space dimension is $D_A = d^{N_A}$.

We apply first to both ρ_{1,A_1} and ρ_{2,A_2} the *same* random unitary $U_A = \otimes_{k=1}^{N_A} U_k$, defined as a product of local random unitaries U_k acting on spins $k = 1, \dots, N_A$ (see Fig. 1). Here, the U_k are sampled independently from a unitary 2-design [29,30] defined on the local Hilbert space \mathbb{C}^d and sent via classical communication to both devices (red arrows in Fig. 1). We now perform for the first and second system projective measurements in a standard (computational) basis $|\mathbf{s}_A\rangle \equiv |s_1, \dots, s_{N_A}\rangle$. Here, \mathbf{s}_A denotes a string of possible measurement outcomes for spins $k = 1, \dots, N_A$. Repeating these measurements for fixed U_A provides us with estimates of the probabilities

$P_U^{(i)}(\mathbf{s}_A) = \text{Tr}_{A_i}[U_A \rho_{i,A_i} U_A^\dagger |\mathbf{s}_A\rangle\langle \mathbf{s}_A|]$ for $i = 1, 2$ (see Fig. 1). In a second step, this procedure is repeated for many different random unitaries U_A .

Finally, we estimate the density matrix overlap $\text{Tr}[\rho_{1,A_1} \rho_{2,A_2}]$ from second-order *cross-correlations* between the two platforms via

$$\text{Tr}[\rho_{i,A_i} \rho_{j,A_j}] = d^{N_A} \sum_{\mathbf{s}_A, \mathbf{s}'_A} (-d)^{-\mathcal{D}[\mathbf{s}_A, \mathbf{s}'_A]} \overline{P_U^{(i)}(\mathbf{s}_A) P_U^{(j)}(\mathbf{s}'_A)}, \quad (2)$$

with $i = 1, j = 2$. This is proven in Supplemental Material [31], Appendix A, using the properties of unitary 2-designs, thus generalizing [17] to cross-platform settings. Here, $\overline{\dots}$ denotes the ensemble average over random unitaries of the form U_A . The Hamming distance $\mathcal{D}[\mathbf{s}_A, \mathbf{s}'_A]$ between two strings \mathbf{s}_A and \mathbf{s}'_A is defined as the number of spins where $s_k \neq s'_k$, i.e., $\mathcal{D}[\mathbf{s}_A, \mathbf{s}'_A] \equiv |\{k \in \{1, \dots, N_A\} | s_k \neq s'_k\}|$. The purities $\text{Tr}[\rho_{1,A_1}^2]$ and $\text{Tr}[\rho_{2,A_2}^2]$ for the first and second subsystem are obtained by setting in Eq. (2) $i = j = 1$ and $i = j = 2$, respectively, i.e., as second-order *autocorrelations* of the probabilities $P_U^{(i)}(\mathbf{s}_A)$ and $P_U^{(i)}(\mathbf{s}'_A)$ [17,28].

We emphasize that the above protocol to measure the cross-platform fidelity of two quantum states requires only classical communication of random unitaries and measurement outcomes between the two platforms, with the experiments possibly taking place at very different points in time and space. In its present form, the protocol requires, or assumes, no prior knowledge of the quantum states. These states can be mixed states, and refer to subsystems, allowing in particular a comparison of subsystem fidelities for various sizes. We note that our protocol can be used to perform fidelity estimation towards known target theoretical states, as an experiment-theory comparison (see below). In this setting, and when the “theory state” is pure, direct fidelity estimation protocols have been developed [8,9], that can be more efficient for certain well-conditioned states, which are supported on a small number of multiqubit Pauli operators.

Scaling of the required number of experimental runs.— In practice, a statistical error of the estimated fidelity arises from a finite number of projective measurements N_M performed per random unitary and a finite number N_U of random unitaries used to infer overlap and purities via Eq. (2). Experimentally relevant is, therefore, the scaling of the total number of experimental runs $N_M N_U$ (the measurement budget), which are required to reduce this statistical error below a fixed value ϵ , for N_A qubits. In addition, there is the optimal allocation of resources, N_U and N_M , for a given measurement budget $N_M N_U$.

In Fig. 2 we present numerical results for the average statistical error as a function of N_M and N_U , and infer the scaling of the measurement budget with (sub)system size N_A . For simplicity, we assume that the target fidelity

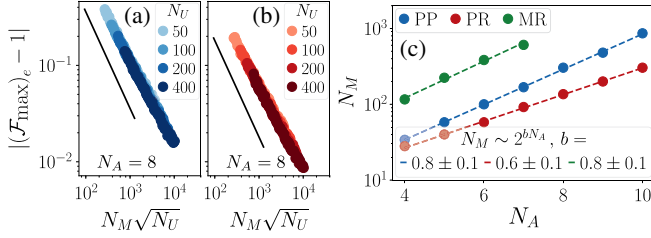


FIG. 2. Scaling of the required number of measurements. (a), (b) Average statistical error $|[\mathcal{F}_{\max}(\rho_A, \rho_A)]_e - 1|$ as a function of the number of measurements N_M per random unitary for various N_U (darkness of colors). The state ρ_A of $N_A = 8$ qubits ($d = 2$) is taken to be (a) a pure product state (PP) and (b) a pure Haar random state (PR). Black lines are guides for the eye, $\sim 1/(N_M\sqrt{N_U})$. (c) Scaling of the minimal number of required measurements N_M to estimate $[\mathcal{F}_{\max}(\rho_A, \rho_A)]_e$ up to a fixed statistical error of 0.05 as a function of the number of qubits N_A , for fixed $N_U = 100$. The mixed random states (MR) are obtained from tracing out 3 qubits from Haar random states of $N_A + 3$ qubits.

$\mathcal{F}_{\max}(\rho_{1,A_1}, \rho_{2,A_2})$ for the two states ρ_{1,A_1} and ρ_{2,A_2} is known and analyze the scaling of the statistical error $|[\mathcal{F}_{\max}(\rho_{1,A_1}, \rho_{2,A_2})]_e - \mathcal{F}_{\max}(\rho_{1,A_1}, \rho_{2,A_2})|$ of an estimated fidelity $[\mathcal{F}_{\max}(\rho_{1,A_1}, \rho_{2,A_2})]_e$. Focusing on experimentally relevant system sizes, we simulate experiments by applying N_U random unitaries to ρ_{1,A_1} and ρ_{2,A_2} and sample independently N_M projective measurements from each state. We then infer an estimation $[\mathcal{F}_{\max}(\rho_{1,A_1}, \rho_{2,A_2})]_e$ of the fidelity $\mathcal{F}_{\max}(\rho_{1,A_1}, \rho_{2,A_2})$ using Eq. (2), and calculate—from many of these numerical experiments—the average statistical error $|[\mathcal{F}_{\max}(\rho_{1,A_1}, \rho_{2,A_2})]_e - \mathcal{F}_{\max}(\rho_{1,A_1}, \rho_{2,A_2})|$. In Fig. 2 we concentrate on the case where the quantum states $\rho_{1,A_1} = \rho_{2,A_2} = \rho_A$ on the two platforms are identical; i.e., the exact fidelity equals $\mathcal{F}_{\max}(\rho_A, \rho_A) = 1$ (for the general case, see Appendix C [31]).

In Figs. 2(a) and 2(b), the average statistical error $|[\mathcal{F}_{\max}(\rho_A, \rho_A)]_e - 1|$ is shown as a function of N_M for a system of $N_A = 8$ qubits ($d = 2$) and various N_U and for two very different types of states ρ_A : (a) pure product states (PP) and (b) pure (entangled) Haar random states (PR) which are obtained by applying a Haar random unitary to a pure product state [31]. Our numerical analysis shows that, in the regime $N_M \lesssim D_A$ and $N_U \gg 1$, $|[\mathcal{F}_{\max}(\rho_A, \rho_A)]_e - 1| \sim 1/(N_M\sqrt{N_U})$. For unit target fidelity, the optimal allocation of the total measurement budget $N_U N_M$ is thus to keep N_U small and fixed [38].

Fixing $N_U = 100$, we display in Fig. 2(c) the scaling of the number of projective measurements N_M per unitary required to determine the fidelity $\mathcal{F}_{\max}(\rho_A, \rho_A)$ up to an average statistical error $|[\mathcal{F}_{\max}(\rho_A, \rho_A)]_e - 1| \leq \epsilon$ below $\epsilon = 0.05$. We find a scaling $N_M \sim 2^{bN_A}$ with $b = 0.8 \pm 0.1$ for PP and $b = 0.6 \pm 0.1$ for PR states, which persists for tested $\epsilon = 0.02, \dots, 0.2$. The fidelity estimation of PR (entangled) states is thus less prone to statistical errors

which we attribute to the fact that fluctuations across random unitaries are reduced due to the mixedness of the subsystems. A similar scaling, with larger prefactor, is found for a mixed random state (MR), obtained from tracing out 3 qubits of a random state of $N_A + 3$ qubits. This is directly related to the smaller overall magnitude of numerator and denominator of the fidelity for mixed states [see Eq. (1)].

We note that the optimal allocation of N_U versus N_M for given $N_U N_M$ depends on the quantum states, in particular, their fidelity and the allowed statistical error ϵ , and is thus *a priori* not known. In practice, an iterative procedure can be applied in which the allocation of measurement resources N_U versus N_M is stepwise inferred from newly acquired data. To this end, the expected reductions of the standard error of the estimated fidelity are calculated, upon increasing either N_U or N_M , using resampling techniques (see Appendix C of Ref. [31]). Accordingly, N_U and N_M are updated iteratively to maximize the expected decrease of statistical uncertainty, until a predefined value of the estimated error is reached.

In summary, we find that the presented protocol requires a total number of experimental runs $N_U N_M \sim 2^{bN_A}$ with $b \lesssim 1$, which is, despite being exponential, significantly less than full QST with exponents $b \geq 2$ [19]. For instance, QST via compressed sensing [19,20] would require at least $\mathcal{O}(2^{2N_A}) \sim 10^6$ experimental runs for a pure 10-qubit state, whereas for our protocol 10^4 (PR) to 10^5 (PP) experimental runs would be sufficient to obtain a fidelity estimation up to a statistical uncertainty of 0.05.

Fidelity estimation with trapped ions.—In the following, we present, as proof of principle, the measurement of experiment-theory fidelities and experiment-experiment fidelities of highly entangled quantum states prepared via quench dynamics in a trapped ion quantum simulator. To this end, we use data presented in Ref. [28]. Here, the entanglement generation after a quantum quench with the XY Hamiltonian,

$$H_{XY} = \hbar \sum_{i < j} J_{ij} (\sigma_i^+ \sigma_j^- + \sigma_i^- \sigma_j^+) + \hbar B \sum_i \sigma_i^z, \quad (3)$$

was experimentally monitored, with σ_i^z the third spin-1/2 Pauli operator, σ_i^+ (σ_i^-) the spin-raising (spin-lowering) operators acting on spin i , and $J_{ij} \approx J_0/|i-j|^\alpha$ the coupling matrix with an approximate power-law decay $\alpha \approx 1.24$ and $J_0 = 420 \text{ s}^{-1}$. The initial Néel-state, $\rho_E(0) \approx |\psi\rangle\langle\psi|$ with $|\psi\rangle = |0, 1, 0, \dots, 1\rangle$ for $N = 10$ ions, was time evolved under H_{XY} into the state $\rho_E(t)$. Subsequently, randomized measurements were performed and, from statistical autocorrelations of the outcome probabilities $P_U^{(E)}(\mathbf{s}_A)$, purity and second-order Rényi entropy of $\rho_E(t)$ (and of density matrices of arbitrary subsystems) were inferred. In total, $N_U = 500$ random unitaries were used and $N_M = 150$ projective measurements per random

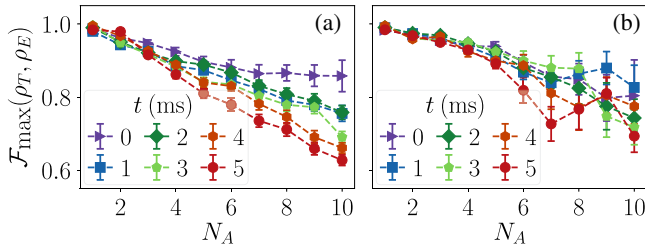


FIG. 3. Experiment-theory verification in a trapped ion quantum simulator. Measured fidelities $\mathcal{F}_{\max}(\rho_E, \rho_T)$ as a function of partition size N_A (total system 10 qubits) for states ρ_E evolved with H_{XY} ($J_0 = 420 \text{ s}^{-1}$, $\alpha = 1.24$) for various times; experimental data from Ref. [28]. Theory states ρ_T are obtained with (a) unitary dynamics and including (b) decoherence effects (see text). In both panels, $N_U = 500$ and $N_M = 150$. Error bars are obtained with bootstrap resampling [39]. Dashed lines are guides for the eye.

unitary were performed. For further experimental details, see Ref. [28].

To numerically simulate the experiment and obtain a corresponding theory state $\rho_T(t)$, we perform exact diagonalization to simulate unitary dynamics or exactly solve a master equation to include decoherence effects. Subsequently, the $N_U = 500$ random unitaries which have been employed in the experiment are applied to $\rho_T(t)$ and the occupation probabilities $P_U^{(T)}(\mathbf{s})$ are calculated exactly for each random unitary.

In Figs. 3(a) and 3(b), experiment-theory fidelities $\mathcal{F}_{\max}(\rho_{E_A}, \rho_{T_A})$ of reduced states of connected partitions [$1 \rightarrow N_A$] are displayed as a function N_A for various times after the quantum quench. For Fig. 3(a), theory states are calculated by simulating unitary dynamics, and for Fig. 3(b), we additionally include decoherence effects, inherent to the state preparation (imperfect initial state preparation, spin flips, and dephasing noise) and the measurement process (depolarizing noise during the random measurement) [28]. In both cases, we find a single qubit fidelity being constant in time and close to unity. With increasing subsystem size and time, the estimated fidelities tend to decrease. Remarkably, we find theory-experiment fidelities (a) $\gtrsim 0.6$ [(b) $\gtrsim 0.7$] even at late times $T = 5$ ms, when the system has undergone complex many-body dynamics and is highly entangled [28].

We observe in Fig. 3 a decrease of the estimated fidelity with system size already at $t = 0$ ms, despite the fact that the initial Néel state can be prepared and, being a simple product state, directly verified (preparation fidelity $\gtrsim 0.97$ for $N_A = 10$). Thus, we attribute the decrease of the estimated theory-experiment fidelity mainly to experimental imperfections in the implementation of the randomized measurements, of two types: (i) unitary errors in the form of random underrotations or overrotations, i.e., a mismatch between the random unitaries applied in experiment and theory, and (ii) decoherence in the form of local

depolarizing noise. While (i) decreases the estimated density matrix overlap, and thus fidelity, in both cases presented in Fig. 3, (ii) is taken into account into the theory state for Fig. 3(b) and thus the estimated fidelities are larger than in Fig. 3(a). We emphasize that both sources of imperfections decrease the estimated fidelity and do not lead to false positives, and we refer for a detailed error modeling and further experimental investigations to Appendix E of Ref. [31].

As a first step towards the cross-platform verification of two quantum devices, we now present experiment-experiment fidelities of quantum states prepared sequentially in the same experiment. To this end, we divide the data obtained in Ref. [28] into two parts, from now on called experiment E_1 and experiment E_2 , each consisting of measurement outcomes for the same $N_U = 500$ random unitaries and $N_M = 75$ measurements per random unitary. Using Eq. (2), we calculate overlap and purities, and from this the fidelity $\mathcal{F}_{\max}(\rho_{E_1}, \rho_{E_2})$. In Figs. 4(a) and 4(b), the experiment-experiment and theory-experiment fidelities are displayed as a function of subsystem size for $t = 0, 1$ ms. In comparison to theory-experiment fidelities, experiment-experiment fidelities are higher for both $t = 0$ ms and $t = 1$ ms. We conclude that the random unitaries are reproducibly prepared in the experiment, with a systematic

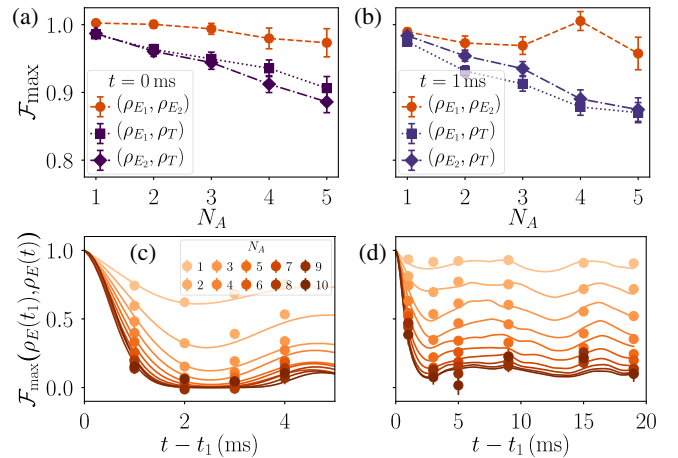


FIG. 4. Experiment self-verification in a trapped ion quantum simulator. (a),(b) Estimated fidelities \mathcal{F}_{\max} of two reduced states ρ_{E_1} and ρ_{E_2} prepared sequentially in the same experiment as a function of partition size, [$1 \rightarrow N_A$]. The states ρ_{E_1} and ρ_{E_2} are (a) two Néel states which have been (b) time evolved under H_{XY} ($J_0 = 420 \text{ s}^{-1}$, $\alpha = 1.24$) to $t = 1$ ms; experimental data from Ref. [28]. Experiment-theory fidelities are obtained by simulating unitary dynamics (see text). Dashed lines are guides for the eye. (c),(d) Measured fidelities $\mathcal{F}_{\max}(\rho_E(t_1), \rho_E(t))$ for states time evolved with H_{XY} as a function of the time difference $t - t_1$ ($t_1 = 1$ ms) for (c) a clean system and (d) with additional disorder (see text). Different colors refer to different partitions [$1 \rightarrow N_A$]. Lines show theory simulations including decoherence effects (see text). In all panels, error bars are estimated with bootstrap resampling [39].

mismatch (unitary error) compared to the ones on the classical computer.

Finally, we illustrate our method in Figs. 4(c) and 4(d) by the measurement of $\mathcal{F}_{\max}(\rho_E(t_1), \rho_E(t))$ of two quantum states evolved for different times. We consider in Fig. 4(c) the clean system, governed by H_{XY} , and in Fig. 4(d) the case where additional on-site disorder $H_{\text{tot}} = H_{XY} + \sum_j \delta_j \sigma_j^z$, with δ_j sampled uniformly from $[-3J_0, 3J_0]$, is added. We find that for the clean system the fidelity decays quickly as a function of the subsystem size and time difference, resembling the complex, ergodic dynamics in the interacting many-body system. On the contrary, for the disordered system the fidelity stays, after an initial short-time decay, approximately constant, and at a finite value even for large (sub)systems. Our results are thus consistent with localization phenomena, characterized through the system's memory of earlier time and slow dynamics, as also studied with out-of-time order correlators [40–43], also accessible with randomized measurements [44].

Conclusion.—We have presented a protocol to perform cross-platform verification of quantum devices by direct fidelity measurements, requiring only classical communication and significantly fewer measurements than full quantum state tomography. Extrapolating the numerically extracted scaling laws for the required number of experimental runs, we expect it to be applicable in state-of-the-art quantum simulators and computers with high repetition rates for (sub)systems consisting of a few tens of qubits. In larger quantum systems, it gives access to the fidelities of all possible subsystems up to a given size—determined by the accepted statistical error and the measurement budget—and thus enables a fine-grained comparison of large quantum systems. Furthermore, we expect that adaptive sampling techniques have the potential to reduce the measurement cost, in particular, when knowledge over the quantum states of interest is taken into account.

We thank B. Kraus, A. Browaeys, J. Bollinger, Z. Cian, J. Emerson, S. Glancy, M. Hafezi, R. Kaubrügger, A. Kaufmann, A. Gorshkov, D. Leibfried, C. Monroe and his group, T. Monz, D. Slichter, A. Rey, A. Wilson, and J. Ye for discussions. The project has received funding from the European Research Council (ERC) under the European Union's Horizon 2020 research and innovation programme (Grant Agreement No. 741541), and from the European Union's Horizon 2020 research and innovation programme under Grant Agreement No. 817482 (Pasquans) and No 731473 (QuantERA via QTFLAG). Furthermore, this work was supported by the Simons Collaboration on Ultra-Quantum Matter, which is a grant from the Simons Foundation (651440, P.Z.). We acknowledge support by the ERC Synergy Grant UQUAM and by the Austrian Science Fund through the SFB BeyondC (F71). Numerical simulations were realized with QuTiP.

- [1] J. Preskill, *Quantum* **2**, 79 (2018).
- [2] J. Eisert, D. Hangleiter, N. Walk, I. Roth, D. Markham, R. Parekh, U. Chabaud, and E. Kashefi, [arXiv:1910.06343](https://arxiv.org/abs/1910.06343).
- [3] J. Emerson, R. Alicki, and K. Życzkowski, *J. Opt. B* **7**, S347 (2005).
- [4] J. Emerson, M. Silva, O. Moussa, C. Ryan, M. Laforest, J. Baugh, D. G. Cory, and R. Laflamme, *Science* **317**, 1893 (2007).
- [5] E. Knill, D. Leibfried, R. Reichle, J. Britton, R. B. Blakestad, J. D. Jost, C. Langer, R. Ozeri, S. Seidelin, and D. J. Wineland, *Phys. Rev. A* **77**, 012307 (2008).
- [6] D. Lu, H. Li, D.-A. Trotter, J. Li, A. Brodutch, A. P. Krismanich, A. Ghavami, G. I. Dmitrienko, G. Long, J. Baugh, and R. Laflamme, *Phys. Rev. Lett.* **114**, 140505 (2015).
- [7] A. Erhard, J. J. Wallman, L. Postler, M. Meth, R. Stricker, E. A. Martinez, P. Schindler, T. Monz, J. Emerson, and R. Blatt, [arXiv:1902.08543](https://arxiv.org/abs/1902.08543).
- [8] M. P. da Silva, O. Landon-Cardinal, and D. Poulin, *Phys. Rev. Lett.* **107**, 210404 (2011).
- [9] S. T. Flammia and Y.-K. Liu, *Phys. Rev. Lett.* **106**, 230501 (2011).
- [10] B. P. Lanyon, C. Maier, M. Holzäpfel, T. Baumgratz, C. Hempel, P. Jurcevic, I. Dhand, A. S. Buyskikh, A. J. Daley, M. Cramer, M. B. Plenio, R. Blatt, and C. F. Roos, *Nat. Phys.* **13**, 1158 (2017).
- [11] Y.-C. Liang, Y.-H. Yeh, P. E. M. F. Mendonça, R. Y. Teh, M. D. Reid, and P. D. Drummond, *Rep. Prog. Phys.* **82**, 076001 (2019).
- [12] R. Jozsa, *J. Mod. Opt.* **41**, 2315 (1994).
- [13] N. M. Linke, D. Maslov, M. Roetteler, S. Debnath, C. Figgatt, K. A. Landsman, K. Wright, and C. Monroe, *Proc. Natl. Acad. Sci. U.S.A.* **114**, 3305 (2017).
- [14] C. Greganti *et al.*, [arXiv:1905.09790](https://arxiv.org/abs/1905.09790).
- [15] S. J. van Enk and C. W. J. Beenakker, *Phys. Rev. Lett.* **108**, 110503 (2012).
- [16] A. Elben, B. Vermersch, M. Dalmonte, J. I. Cirac, and P. Zoller, *Phys. Rev. Lett.* **120**, 050406 (2018).
- [17] A. Elben, B. Vermersch, C. F. Roos, and P. Zoller, *Phys. Rev. A* **99**, 052323 (2019).
- [18] H. Häffner *et al.*, *Nature (London)* **438**, 643 (2005).
- [19] D. Gross, Y. K. Liu, S. T. Flammia, S. Becker, and J. Eisert, *Phys. Rev. Lett.* **105**, 150401 (2010).
- [20] C. Riofrío, D. Gross, S. Flammia, T. Monz, D. Nigg, R. Blatt, and J. Eisert, *Nat. Commun.* **8**, 15305 (2017).
- [21] G. Torlai, G. Mazzola, J. Carrasquilla, M. Troyer, R. Melko, and G. Carleo, *Nat. Phys.* **14**, 447 (2018).
- [22] A. C. Keith, C. H. Baldwin, S. Glancy, and E. Knill, *Phys. Rev. A* **98**, 042318 (2018).
- [23] G. Carleo, I. Cirac, K. Cranmer, L. Daudet, M. Schuld, N. Tishby, L. Vogt-Maranto, and L. Zdeborová, [arXiv:1903.10563](https://arxiv.org/abs/1903.10563) [Rev. Mod. Phys. (to be published)].
- [24] Our protocol assumes only classical communication between platforms 1 and 2. Existence of a quantum link would allow quantum state transfer and provide, in principle, an efficient quantum protocol for $\text{Tr}[\rho_1 \rho_2]$ [25–27].
- [25] A. J. Daley, H. Pichler, J. Schachenmayer, and P. Zoller, *Phys. Rev. Lett.* **109**, 020505 (2012).
- [26] R. Islam, R. Ma, P. M. Preiss, M. E. Tai, A. Lukin, M. Rispoli, and M. Greiner, *Nature (London)* **528**, 77 (2015).

- [27] N. M. Linke, S. Johri, C. Figgatt, K. A. Landsman, A. Y. Matsuura, and C. Monroe, *Phys. Rev. A* **98**, 052334 (2018).
- [28] T. Brydges, A. Elben, P. Jurcevic, B. Vermersch, C. Maier, B. P. Lanyon, P. Zoller, R. Blatt, and C. F. Roos, *Science* **364**, 260 (2019).
- [29] D. Gross, K. Audenaert, and J. Eisert, *J. Math. Phys. (N.Y.)* **48**, 052104 (2007).
- [30] C. Dankert, R. Cleve, J. Emerson, and E. Livine, *Phys. Rev. A* **80**, 012304 (2009).
- [31] See Supplemental Material at <http://link.aps.org/supplemental/10.1103/PhysRevLett.124.010504> for [brief description], which includes Refs. [32–37].
- [32] J. Watrous, *The Theory of Quantum Information* (Cambridge University Press, Cambridge, England, 2018).
- [33] D. A. Roberts and B. Yoshida, *J. High Energy Phys.* **04** (2017) 121.
- [34] Y. Nakata, C. Hirche, M. Koashi, and A. Winter, *Phys. Rev. X* **7**, 021006 (2017).
- [35] B. Vermersch, A. Elben, M. Dalmonte, J. I. Cirac, and P. Zoller, *Phys. Rev. A* **97**, 023604 (2018).
- [36] H. Hotelling, *J. R. Stat. Soc.* **15**, 193 (1953).
- [37] F. Haake, *Quantum Signatures of Chaos*, Vol. 54 (Springer, Berlin & Heidelberg, 2010).
- [38] To allow for estimation of the statistical uncertainty of estimated fidelity a minimal number of $N_U \gg 1$ is required.
- [39] B. Efron and G. Gong, *Am. Stat.* **37**, 36 (1983).
- [40] M. Serbyn and D. A. Abanin, *Phys. Rev. B* **96**, 014202 (2017).
- [41] R. Fan, P. Zhang, H. Shen, and H. Zhai, *Science bulletin* **62**, 707 (2017).
- [42] X. Chen, T. Zhou, D. A. Huse, and E. Fradkin, *Ann. Phys. (Amsterdam)* **529**, 1600332 (2017).
- [43] Y. Huang, Y.-L. Zhang, and X. Chen, *Ann. Phys. (Amsterdam)* **529**, 1600318 (2017).
- [44] B. Vermersch, A. Elben, L. M. Sieberer, N. Y. Yao, and P. Zoller, *Phys. Rev. X* **9**, 021061 (2019).